AAC Journals.ASM.org

A Novel Y319H Substitution in CYP51C Associated with Azole Resistance in *Aspergillus flavus*

R. A. Paul,[a] S. M. Rudramurthy,[a] J. F. Meis,[b,c] J. W. Mouton,[b,c] A. Chakrabarti[a]

Department of Medical Microbiology, Postgraduate Institute of Medical Education and Research, Chandigarh, India[a]; Department of Medical Microbiology and Infectious Diseases, Canisius Wilhelmina Hospital, Nijmegen, The Netherlands[b]; Department of Medical Microbiology and Infectious Diseases, Erasmus MC, Rotterdam, The Netherlands[c]

This study aimed to explore any mutation in the *CYP51* gene conferring azole resistance in *Aspergillus flavus*. Two voriconazole-resistant and 45 voriconazole-susceptible isolates were included in the study. Sequence analysis demonstrated a T1025C nucleotide change in *CYP51C*, resulting in the Y319H amino acid substitution in one resistant isolate. However, the earlier described T788G mutation in *CYP51C* conferring voriconazole resistance in *A. flavus* isolates was present in all isolates, irrespective of their susceptibility status.

Aspergillus flavus is the second leading cause of invasive aspergillosis in immunocompromised patients and the predominant causative agent of fungal rhinosinusitis and fungal eye infections (endophthalmitis and keratitis) in tropical countries, like India, Sudan, Kuwait, and Iran (1–8). Voriconazole is used primarily to treat infections caused by *A. flavus*. Long-term azole therapy may predispose *A. flavus* to acquire resistance to azoles, including voriconazole

Lanosterol 14 α-demethylase (LDM), which catalyzes the rate-limiting step in the ergosterol biosynthetic pathway, serves as the primary target for azole antifungal drugs. The mechanism of azole resistance in *Aspergillus fumigatus* is well studied. Missense mutations and alteration of *cis* regulatory regions in the LDM coding gene *CYP51A* have been found to be the dominant mechanisms of azole resistance in *A. fumigatus* (9–12), whereas studies to evaluate the mechanism of azole resistance in *A. flavus* are sparse (13–15). The present study is an attempt to understand the mechanism of azole resistance in *A. flavus*.

Two non-wild-type (non-WT) clinical isolates of *A. flavus*, NCPPF 761157 and NCCPF 760815, with higher MIC values for voriconazole than for the respective wild-type (WT) cutoff value, and 4 WT isolates were initially used (Table 1). The wild type and non-wild type were defined on the basis of epidemiological cutoff values (ECV), with the non-WT having a voriconazole MIC of >1 μg/ml and WT with a voriconazole MIC of ≤1 μg/ml (16). The non-WT strain, NCCPF 761157, was isolated from a sputum sample from a patient with chronic obstructive pulmonary disease, and NCCPF 760815 was isolated from a nasal tissue sample from a patient from India having granulomatous fungal rhinosinusitis. Forty-five additional WT *A. flavus* clinical isolates were included to screen and validate the mutations (single-nucleotide polymorphisms [SNPs] and indels). Identification of the isolates was done by sequencing partial β-tubulin and calmodulin genes using primers bt2a (GGTAACCAAATCGGTGCTGCTTTC) and bt2b (ACCCTCAGTGTAGTGACCCTTGGC), and cmdA7 (GCCAAA ATCT TCATCCGTAG) and cmdA8 (ATTTCGTTCAGAATGCC AGG) (17, 18). Antifungal susceptibility testing was done as per CLSI and EUCAST guidelines (19–22). Coding sequences of the close homologues of *CYP51A* of *A. fumigatus* in *A. flavus*, namely *CYP51A* (GenBank accession no. XM_002375082.1), *CYP51B* (GenBank accession no. XM_002379089.1), and *CYP51C* (GenBank accession no. XM_002383890.1), were downloaded from GenBank (http://www.ncbi.nlm.nih.gov/GenBank), as mentioned by Liu et al. (15). Overlapping primer sets were designed for each homologue, and PCR amplification of each open reading frame and the upstream and downstream regions of each homologue was performed (Table 2). To reduce errors during amplification, two different high-fidelity DNA polymerases (Platinum Taq; Life Technologies, Carlsbad, CA, and KOD Plus-; Toyobo Life Science Department, Osaka, Japan) were used in different sets of experiments (twice). Sequence amplification and analysis were performed using the BigDye Terminator ready reaction kit and a genetic analyzer (Applied Biosystems, Foster City, CA). Consensus of the forward and reverse sequences and the contig assembly of each product from the overlapping fragments were done using the BioNumerics software (Applied Maths, Ghent, Belgium). Sequences were aligned in Clustal X2, and amino acid sequences were deduced using the ExPASy online tool (http://www.expasy.org/translate). To assess the impact of the Y319H substitution on the general structure of *A. flavus* CYP51C, homology modeling and molecular dynamic simulations were performed for the WT and the Y319H mutant. The amino acid sequence of the query protein was downloaded from UniProt protein sequence database (UniProt ID I8TEB1). The three-dimensional (3D) homology models of the WT and Y319H mutant were generated using the Swiss-Model (http://swissmodel.expasy.org/interactive#sequence) workspace. The LDM (PDB ID 4K0F) structure sharing a sequence identity of 50.51% was used as the template for model building. Models were validated using the Qmean4 score. A production dynamic simulation run was performed using Gromacs 4.6.5 with

Received 17 March 2015 Returned for modification 4 May 2015
Accepted 10 July 2015
Accepted manuscript posted online 27 July 2015
Citation Paul RA, Rudramurthy SM, Meis JF, Mouton JW, Chakrabarti A. 2015. A novel Y319H substitution in CYP51C associated with azole resistance in *Aspergillus flavus*. Antimicrob Agents Chemother 59:6615–6619. doi:10.1128/AAC.00637-15.
Address correspondence to A. Chakrabarti, arunaloke@hotmail.com.

doi:10.1128/AAC.00637-15

TABLE 1 Antifungal susceptibility profile of *A. flavus* isolates for various drugs, performed using CLSI M38-A2 (19)

Strain	MIC/MEC (μg/ml) for[a]:						
	AMB	VOR[b]	ITR	POS	CSP	MCF	ANI
NCCPF 761157	2	4 (8)	16	0.25	0.03	0.015	0.0075
NCCPF 760815	4	2 (2)	1	0.5	4	0.12	0.25
NCCPF 760816	2	0.5 (1)	0.12	0.12	0.06	0.015	0.06
NCCPF 760690	4	0.125 (0.25)	0.06	0.03	0.03	0.015	0.06
NCCPF 761379	1	0.5	0.12	0.06	0.06	0.015	0.06
NCCPF 761425	4	0.5	0.25	0.12	0.03	0.015	0.06

[a] MEC, minimum effective concentration of echinocandins; AMB, amphotericin B; VOR, voriconazole; ITR, itraconazole; POS, posaconazole; CSP, caspofungin; MCF, micafungin; ANI, anidulafungin.
[b] Values in parentheses for voriconazole are MICs determined by EUCAST method, E.DEF 9.1 (20).

the GROMOS96 43a1 force field. Molecular dynamics (MD) trajectory analysis was performed using Gromacs utilities, and all the graphs were plotted using Grace. To study the structural and functional effects of the Y319H substitution, the WT and non-WT CYP51C were also analyzed on HOPE (23).

A comparison of the nucleotide and amino acid sequences of *CYP51A* homologs of non- WT (NCCPF 761157 and NCCPF 760815) and WT strains (760816, 760690, 760425, and 760379) of *A. flavus* with a reference sequence (*A. flavus* strain NRRL3357) showed the G680A transition in *CYP51A* of strain NCCPF 761157, resulting only in the amino acid change A205T. The upstream (−1,000 bp) and downstream (+1,000 bp) regulatory regions were intact in all strains. In addition, there was no change in the nucleotide or amino acid sequences in CYP51B. However, *CYP51C* was most polymorphic in nature (Table 3). Six missense nucleotide changes and the resulting amino acid replacements were detected in CYP51A and CYP51C. However, 5 of these substitutions (A205T, M54T, S240A, D254N, and I285V) did not appear to affect the azole susceptibility of the organism, as these changes were also found in WT isolates. Only one nonsynonymous mutation, T1025C, translating to Y319H, was found to be specific to a non-WT isolate (NCCPF 761157). To confirm these

TABLE 2 Primers used in the study for amplification of homologs of *CYP51*

CYP51 homolog	Primer name	Primer sequence (5′–3′)	Position on coordinate (bases)
CYP51A	AflaCYP51A F1	CAAGAACAGCCTGCACAGAG	324
	AflaCYP51AR1	GGGTGGATCAGTCTTATTA	1126
	AflaCYP51AF2	GCAATCATCGTCCTAAATC	1066
	AflaCYP51AR2	CTGTCCATTCTTGTAGGTA	1899
	AflaCYP51AF3	GCATGAGGGAGATCTATATG	1791
	AflaCYP51AR3	CCTATAATTGCTGGTTTCG	2649
	AflaCYP51AF4	TGAAGCTATTCAATGTAGAC	2480
	AflaCYP51AR4	ACTGCTGATGGTGTGCTAAG	3358
	A205T-F	GGAGTCGCATGTACCATTGA	1510
	A205T-R	TGAAGTTGATCGGAGTGAACC	1716
CYP51B	AflaCYP51B F1	AACACGACTAGGAGCTACAC	4182
	AflaCYP51BR1	CACCAATCCACTCTATC	5082
	AflaCYP51BF2	GATCAGGGAAATGTTCTTC	4948
	AflaCYP51BR2	ACGATCGCTGAGATTAC	5620
	AflaCYP51BF3	GTTCAGCAAATGTCGAG	5550
	AflaCYP51BR3	CCTTTCGTCTACCTGTT	6344
	AflaCYP51BF4	AGTGGAGAGCATCCATAGTGA	6231
	AflaCYP51BR4	ACAACCCGTTCAAGATATCGG	7339
CYP51C	AflaCYP51CF1	CTGTTGCAGAGCCGTTGATG	33
	AflaCYP51CR1	CAAAGAGCGACACATAAG	860
	AflaCYP51CF2	GGTAATGTCTGGTCATAGG	751
	AflaCYP51CR2	ATGAGCTTGGAATTGGG	1453
	AflaCYP51CF3	CGAATTCATCCTCAATGG	1336
	AflaCYP51CR3	GTCTCTCGGATCACATT	2137
	AflaCYP51CF4	GGAACTCTACCAAGAGCA	2018
	AflaCYP51CR4	CCTAGATACAGCTAGATACCC	2819
	AflaCYP51Cdel-F	CCAGCGCTCATAGGTGTATT	2634
	AflaCYP51Cdel-R	CGTGGTCAGTCAATTGGGTA	3102
	SNP-F	GCGGTTCTCTACCACGATTTG	677
	SNP-R	AGGGTCTCTCGGATCACATTT	1120

TABLE 3 Mutational analysis of *CYP51A*, *CYP51B*, and *CYP51C* and the corresponding amino acid changes in lanosterol 14 α-demethylase in resistant and sensitive isolates

Strain	Mutations in *CYP51*			Amino acid change in LDM[a]			Regulatory region of *CYP51C*
	CYP51A	*CYP51B*	*CYP51C*	*CYP51A*	*CYP51B*	*CYP51C*	
NCCPF 761157	G680A	None	T161C T788G G830A G923A T1025C	A205T	None	M54T S240A D254N I285V Y319H	4-bp deletion at bp 2734 at bp 2734
NCCPF 760815	None	None	T161C T788G G830A G923A	None	None	M54T S240A D254N I285V	4-bp deletion at bp 2734
NCCPF 760816	None	None	T161C T788G	None	None	M54T S240A	None
NCCPF 760690	None	None	T161C T788G	None	None	M54T S240A	None
NCCPF 761379	None	None	T161C	None	None	M54T S240A	None
NCCPF 761425	None	None	T788G	None	None	M54T S240A	None

[a] LDM, lanosterol 14 α-demethylase.

findings, we used 45 wild-type isolates to screen for the SNPs and indels coding for these phenotypes of *CYP51C* in azole-sensitive strains. Tandem duplication of a promoter sequence, TR 34, along with the nonsynonymous point mutation L98H was reported for azole resistance in clinical and environmental isolates of *A. fumigatus*. However, a mutation of this characteristic was not found in our azole-resistant *A. flavus* isolates. Nonetheless, a 4-bp deletion was found in the AT-rich intergenic region downstream at position 2734 of *CYP51C*, which upon screening of the WT collection showed that it was not related to the resistant phenotype. Instead, a compensatory 4-bp insertion mutation was found in the nearby region in those isolates that harbored this deletion (data not shown). Indel mutations usually arise in intergenic regions, which act as mutational hot spots for indels and play a role in purifying selection (24). The present study also contradicts the finding of Liu et al. (15), in which the T788G mutation was implicated in mediating voriconazole resistance in *A. flavus*. This mutation was not related to voriconazole resistance in our strains, as this SNP was found in all 47 strains tested, irrespective of their susceptibility. Possibly, the T788G mutation is simply a geographical strain variation, as the investigators compared the *CYP51C* sequence of their resistant strain with the *A. flavus* NRRL3357 reference sequence only. Alignment of orthologues of cytochrome P450 of different fungal species and of humans showed substitutions, including A205T, M54T, S240A, D254N, and I285V, which were not present in the conserved motifs. (Table 3). The location of the Y319H substitution in a highly conserved position of *CYP51C* suggests that this might be one of the reasons for azole resistance in our resistant isolates.

As the Y319H substitution is located far from the iron-porphyrin complex, it appears that the substitution indirectly affects drug binding instead of having a direct effect on the docking of azoles at the binding site (Fig. 1). MD simulations revealed that this mutation increases conformational flexibility, as indicated by increased root mean square deviation values (Fig. 2A) and root mean square fluctuation (RMSF) (Fig. 2B); there was a simultaneous decrease

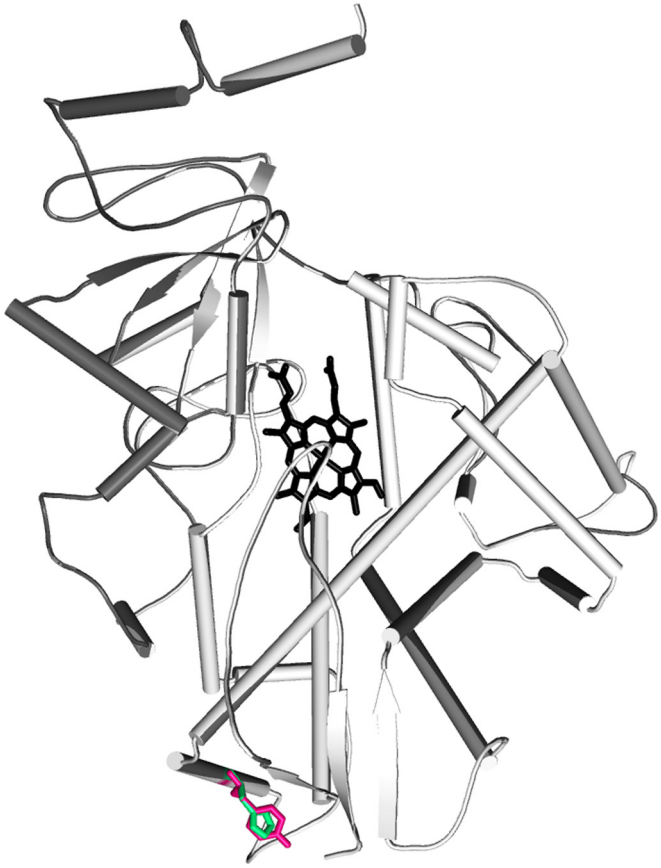

FIG 1 Modeled structure of CYP51C of *A. flavus* shown in cartoon representation. The porphyrin ring is shown in stick representation in black. The tyrosine residue present in the wild type and the histidine in the mutant are shown in hot pink and green, respectively.

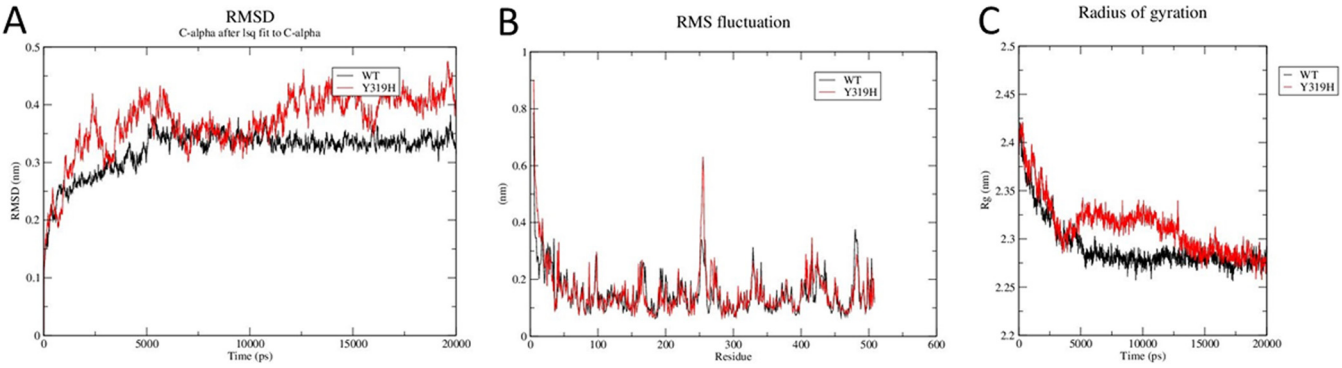

FIG 2 (A) Root mean square deviations of Cα backbones of WT and mutant CYP51C proteins as a function of time (20 ns). (B) Graph shows the average fluctuation of Cα atoms for each residue around the average structure of the protein. The black line stands for the WT molecular dynamics trajectory and the red line for the Y319H mutant dynamics trajectory. (C) Radius of gyration (Rg) of Cα of WT and CYP51C mutant protein as a function of time at 20 ns.

in globularity, as depicted by the increase in the radius of gyration of the mutant protein (Fig. 2C). Differences in the radius of gyration between the WT and non-WT *CYP51C* may be due to a loss of noncovalent interactions, which was caused by the substitution of tyrosine with histidine in the mutant strain. The WT tyrosine residue forms a hydrogen bond with the valine at position 329 and salt bridges with the valine at position 329 and glutamic acid at position 328. Increased flexibility in the non-WT *CYP51C* may be due to the polar nature of histidine causing interatomic repulsions. On the other hand, tyrosine present in the wild type can form hydrophobic interactions, accounting for the lower RMSF. The structural data for the CYP51C protein of *A. flavus* is not available to infer the effect of point mutations on the conformations of drug entry channels of orthologous proteins. However, a similar strategy has been applied in earlier studies (25–28). The results from our study provide clues that increased conformational flexibility in the Y319H mutant may be the reason for its reduced drug binding affinity.

However, the Y319H substitution was not found in the other resistant isolate (NCCPF 760815). The absence of the Y319H substitution in NCCPF 760815 may be due to other mechanisms responsible for the elevated MICs in this isolate. Nonetheless, our findings need to be evaluated in more non-WT *A. flavus* isolates and by producing a Y319H mutant in a WT background and confirming its azole resistance.

Nucleotide sequence accession numbers. The nucleotide sequences of *CYP51C* of NCCPF 761157 and NCCPF 760815 have been submitted to GenBank with the nucleotide accession numbers KR822399 and KR822400, respectively.

ACKNOWLEDGMENTS

We acknowledge the help of Khurram Mushtaq of the Institute of Microbial Technology, Chandigarh, India, during the simulation study and Indian Council of Medical Research for the financial support in conducting the study.

REFERENCES

1. **Pasqualotto AC.** 2009. Differences in pathogenicity and clinical syndromes due to *Aspergillus fumigatus* and *Aspergillus flavus*. Med Mycol **47**(Suppl 1)**:**S261–S270.
2. **Hedayati MT, Pasqualotto AC, Warn PA, Bowyer P, Denning DW.** 2007. *Aspergillus flavus*: human pathogen, allergen and mycotoxin producer. Microbiology **153:**1677–1692. http://dx.doi.org/10.1099/mic.0.2007/007641-0.
3. **Krishnan S, Manavathu EK, Chandrasekar PH.** 2009. *Aspergillus flavus*: an emerging non-*fumigatus Aspergillus* species of significance. Mycoses **52:**206–222. http://dx.doi.org/10.1111/j.1439-0507.2008.01642.x.
4. **Chakrabarti A, Shivaprakash MR, Singh R, Tarai B, George VK, Fomda BA, Gupta A.** 2008. Fungal endophthalmitis: fourteen years' experience from a center in India. Retina **28:**1400–1407. http://dx.doi.org/10.1097/IAE.0b013e318185e943.
5. **Chakrabarti A, Rudramurthy SM, Panda N, Das A, Singh A.** 2015. Epidemiology of chronic fungal rhinosinusitis in rural India. Mycoses **58:**294–302. http://dx.doi.org/10.1111/myc.12314.
6. **Chakrabarti A, Singh R.** 2011. The emerging epidemiology of mould infections in developing countries. Curr Opin Infect Dis **24:**521–526. http://dx.doi.org/10.1097/QCO.0b013e32834ab21e.
7. **Khan ZU, Sanyal SC, Mokaddas E, Vislocky I, Anim JT, Salama AL, Shuhaiber H.** 1997. Endocarditis due to *Aspergillus flavus*. Mycoses **40:**213–217. http://dx.doi.org/10.1111/j.1439-0507.1997.tb00217.x.
8. **Khan ZU, Ahmad S, Mokaddas E, Said T, Nair MP, Halim MA, Nampoory MR, McGinnis MR.** 2007. Cerebral aspergillosis diagnosed by detection of *Aspergillus flavus*-specific DNA, galactomannan and (1→3)-beta-D-glucan in clinical specimens. J Med Microbiol **56:**129–132. http://dx.doi.org/10.1099/jmm.0.46549-0.
9. **Verweij PE, Snelders E, Kema GH, Mellado E, Melchers WJ.** 2009. Azole resistance in *Aspergillus fumigatus*: a side-effect of environmental fungicide use? Lancet Infect Dis **9:**789–795. http://dx.doi.org/10.1016/S1473-3099(09)70265-8.
10. **Chowdhary A, Kathuria S, Xu J, Meis JF.** 2013. Emergence of azole-resistant *Aspergillus fumigatus* strains due to agricultural azole use creates an increasing threat to human health. PLoS Pathog **9:**e1003633. http://dx.doi.org/10.1371/journal.ppat.1003633.
11. **Chowdhary A, Kathuria S, Randhawa HS, Gaur SN, Klaassen CH, Meis JF.** 2012. Isolation of multiple-triazole-resistant *Aspergillus fumigatus* strains carrying the TR/L98H mutations in the *cyp51A* gene in India. J Antimicrob Chemother **67:**362–366. http://dx.doi.org/10.1093/jac/dkr443.
12. **Howard SJ, Cerar D, Anderson MJ, Albarrag A, Fisher MC, Pasqualotto AC, Laverdiere M, Arendrup MC, Perlin DS, Denning DW.** 2009. Frequency and evolution of azole resistance in *Aspergillus fumigatus* associated with treatment failure. Emerg Infect Dis **15:**1068–1076. http://dx.doi.org/10.3201/eid1507.090043.
13. **Krishnan-Natesan S, Chandrasekar PH, Alangaden GJ, Manavathu EK.** 2008. Molecular characterisation of *CYP51A* and *CYP51B* genes coding for P450 14alpha-lanosterol demethylases A (CYP51Ap) and B (CYP51Bp) from voriconazole-resistant laboratory isolates of *Aspergillus flavus*. Int J Antimicrob Agents **32:**519–524. http://dx.doi.org/10.1016/j.ijantimicag.2008.06.018.
14. **Natesan SK, Lamichchane AK, Swaminathan S, Wu W.** 2013. Differential expression of ATP-binding cassette and/or major facilitator superfamily class efflux pumps contributes to voriconazole resistance in *Aspergillus flavus*. Diagn Microbiol Infect Dis **76:**458–463. http://dx.doi.org/10.1016/j.diagmicrobio.2013.04.022.
15. **Liu W, Sun Y, Chen W, Liu W, Wan Z, Bu D, Li R.** 2012. The T788G mutation in the *cyp51C* gene confers voriconazole resistance in *Aspergillus*

flavus causing aspergillosis. Antimicrob Agents Chemother **56:**2598–2603. http://dx.doi.org/10.1128/AAC.05477-11.
16. **Pfaller M, Boyken L, Hollis R, Kroeger J, Messer S, Tendolkar S, Diekema D.** 2011. Use of epidemiological cutoff values to examine 9-year trends in susceptibility of *Aspergillus* species to the triazoles. J Clin Microbiol **49:**586–590. http://dx.doi.org/10.1128/JCM.02136-10.
17. **Glass NL, Donaldson GC.** 1995. Development of primer sets designed for use with the PCR to amplify conserved genes from filamentous ascomycetes. Appl Environ Microbiol **61:**1323–1330.
18. **Geiser DM, Pitt JI, Taylor JW.** 1998. Cryptic speciation and recombination in the aflatoxin-producing fungus *Aspergillus flavus*. Proc Natl Acad Sci U S A **95:**388–393. http://dx.doi.org/10.1073/pnas.95.1.388.
19. **CLSI.** 2008. Reference method for broth dilution antifungal susceptibility testing of filamentous fungi. Approved standard; 2nd ed. CLSI document M38-A2. Clinical and Laboratory Standards Institute, Wayne, PA.
20. **EUCAST.** 2008. EUCAST definitive document E.DEF 9.1: method for the determination of broth dilution minimum inhibitory concentrations of antifungal agents for conidia forming moulds. European Committee on Antimicrobial Susceptibility Testing, Växjö, Sweden. http://www.eucast.org/fileadmin/src/media/PDFs/4ESCMID_Library/3Publications/EUCAST_Documents/Other_Documents/EUCAST_moulds_DEFINITIVE_document_V_ISO_April_08%20final.pdf.
21. **Shivaprakash MR, Geertsen E, Chakrabarti A, Mouton JW, Meis JF.** 2011. *In vitro* susceptibility of 188 clinical and environmental isolates of *Aspergillus flavus* for the new triazole isavuconazole and seven other antifungal drugs. Mycoses **54:**e583–e589. http://dx.doi.org/10.1111/j.1439-0507.2010.01996.x.
22. **Rudramurthy SM, Chakrabarti A, Geertsen E, Mouton JW, Meis JF.** 2011. *In vitro* activity of isavuconazole against 208 *Aspergillus flavus* isolates in comparison with 7 other antifungal agents: assessment according to the methodology of the European Committee on Antimicrobial Susceptibility Testing. Diagn Microbiol Infect Dis **71:**370–377. http://dx.doi.org/10.1016/j.diagmicrobio.2011.08.006.
23. **Venselaar H, Te Beek TA, Kuipers RK, Hekkelman ML, Vriend G.** 2010. Protein structure analysis of mutations causing inheritable diseases. An e-Science approach with life scientist friendly interfaces. BMC Bioinformatics **11:**548.
24. **Williams LE, Wernegreen JJ.** 2013. Sequence context of indel mutations and their effect on protein evolution in a bacterial endosymbiont. Genome Biol Evol **5:**599–605. http://dx.doi.org/10.1093/gbe/evt033.
25. **Snelders E, Karawajczyk A, Verhoeven RJ, Venselaar H, Schaftenaar G, Verweij PE, Melchers WJ.** 2011. The structure-function relationship of the *Aspergillus fumigatus cyp51A* L98H conversion by site-directed mutagenesis: the mechanism of L98H azole resistance. Fungal Genet Biol **48:**1062–1070. http://dx.doi.org/10.1016/j.fgb.2011.08.002.
26. **Wang J, Ma C, Fiorin G, Carnevale V, Wang T, Hu F, Lamb RA, Pinto LH, Hong M, Klein ML, DeGrado WF.** 2011. Molecular dynamics simulation directed rational design of inhibitors targeting drug-resistant mutants of influenza A virus M2. J Am Chem Soc **133:**12834–12841. http://dx.doi.org/10.1021/ja204969m.
27. **Kumar A, Purohit R.** 2014. Use of long term molecular dynamics simulation in predicting cancer associated SNPs. PLoS Comput Biol **10:**e1003318. http://dx.doi.org/10.1371/journal.pcbi.1003318.
28. **Natarajan K, Senapati S.** 2012. Understanding the basis of drug resistance of the mutants of αβ-tubulin dimer via molecular dynamics simulations. PLoS One **7:**e42351. http://dx.doi.org/10.1371/journal.pone.0042351.